

Antibacterial Cephalosporin as Inhibitors for the Corrosion of Iron in Hydrochloric Acid Solutions

M. Abdallah^{1,3}, I.Zaafarany¹, J.H. Al-Fahemi¹, Y.Abdallah² and A.S. Fouda²

¹ Department of Chemistry, Faculty of Applied Science, Umm Al-Qura University, Makkah Al Mukaramha, Saudi Arabia.

² Department of Chemistry, Faculty of Science, El-Mansoura University, El Mansoura- EGYPT.

³ Previous address: Department of Chemistry, Faculty of Science, Benha University, Benha, EGYPT.

*E-mail: metwally555@yahoo.com

Received: 15 June 2012 / Accepted: 2 July 2012 / Published: 1 August 2012

The inhibition efficiency of the antibacterial cephalosporin e.g. cefotaxime, cefalexin, cefradine and cefazolin toward the corrosion of iron in 1.0 M HCl was investigated using electrochemical techniques. The results of these techniques indicated that the inhibition efficiency increased with the concentration of inhibitor but decreased with temperature. Potentiodynamic studies proved that the inhibitors act as mixed mode of inhibition and the inhibitor molecules adsorb on the metal-solution interface. The adsorption of the inhibitors on iron surface obeys the Langmuir adsorption isotherm equation. All impedance spectra in EIS tests exhibit one capacitive loop which indicates that the corrosion reaction is controlled by charge transfer process. Inhibition efficiencies obtained from Tafel polarization, charge transfer resistance (R_{ct}) is consistent.

Keywords: iron, antibacterial cephalosporin, inhibitors, adsorption

1. INTRODUCTION

One of the most important considerations in any industry is the reduction in overall cost in protection and maintenance of materials used. Because iron is the back bone of industrial consideration, the inhibition of the iron corrosion in acid solutions using organic inhibitors has been studied in considerable detail. Acids are widely used in many industries. Some of the important areas of application are industrial acid cleaning, pickling, decaling and in acidization of oil wells [1]. The existing data show that organic inhibitors act by the adsorption and protect the metal by film formation. Organic compounds bearing heteroatom's with high electron density such as

phosphor, sulphur, nitrogen, oxygen or those containing multiple bonds which are considered as adsorption centers, are effective as corrosion inhibitors [2-10]

These investigated inhibitors are classified as the first generation of cephalosporin and were found to have good activity against gram-positive bacteria and relatively moderate activity against gram-negative microorganisms [11]. No data are recorded in the literature about the behavior of this investigated cephalosporin as inhibitors for metallic corrosion. Most of the data recorded in the literature were about the electro analytical behavior of this investigated cephalosporin. These inhibitors were selected as inhibitors because: They are nontoxic, relatively cheap, and easy to produce in purities with proportion of more than 99 % and they are rich in donating atoms such as -N, -O and -S atoms.

Continuation to our goal for searching for safe, ecofriendly and non-toxic corrosion inhibitors, this work aims to investigate the inhibitive action of cephalosporin (which is a safe compound) towards the corrosion of iron in 1.0M HCl using potentiodynamic and electrochemical impedance spectroscopy (EIS) techniques.

2. EXPERIMENTAL

2.1. Working electrode

An iron rod was served as working electrode. The bottom end of the rod specimen with a mean surface area 0.52 cm^2 was polished with different emery papers up to 600 grades, degreased with acetone and finally washed with second distilled water.

2.2. Inhibitors

The following four cephalosporin antibiotics (cefotaxime, cefalexin, cefradine and cefazolin) were kindly provided from Misr Company for Pharmaceuticals and Chemical Industries, Egypt and were used as received without further purification. Their structures are presented in Table 1.

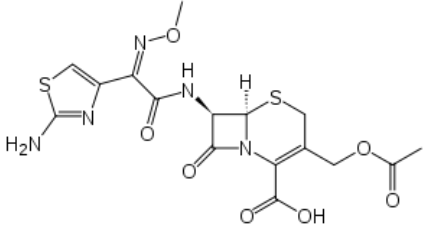
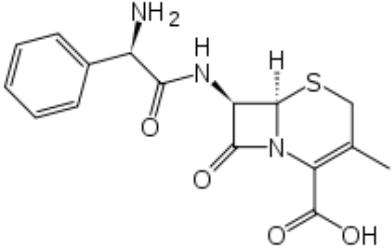
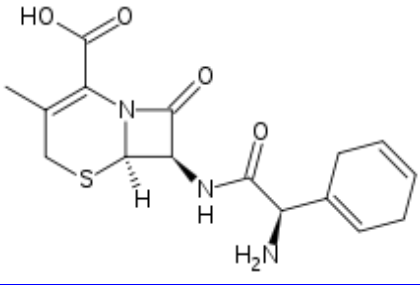
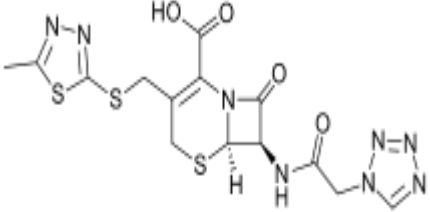
2.3. Solutions

Stock solutions (1000 ppm) of these inhibitors were prepared by dissolving the appropriate weight (1 gram) of each compound separately in bidistilled water in 100 ml measuring flask, then the required concentrations (10, 20, 30, 40, 50 and 60 ppm) were prepared by dilution with doubly distilled water. The aggressive solutions (HCl) used were made of analytical reagent grade. Stock solution of the acid (5 M) was prepared using bidistilled water and this concentration was checked using standard solution of Na_2CO_3 . From this stock concentrated solution, exactly 1 M HCl were prepared by dilution with bidistilled water, which was used throughout experiments for the preparation of solutions.

Measurements were carried out in a three-compartment electrochemical cell. The counter electrode was a platinum sheet of large surface area. The reference electrode was a saturated calomel

electrode (SCE) to which all potentials are referred. The SCE was connected to the main compartment via a Luggin capillary. The cell was water-jacketed and was connected to an ultra thermostat at 25 °C. The electrode potential was allowed to stabilize for 60 min before starting the measurements. For potentiodynamic polarization measurements the corrosion current density (j_{corr}) is determined, which is a measure of corrosion rate.

Table 1. Chemical structures, names and molecular weights of cephalosporin

Inh.	Structure	Name	Molecular Weight
1		Cefotaxime (6R,7R,Z)-3-(acetoxymethyl)-7-(2-(2-aminothiazol-4-yl)-2-(methoxyimino)acetamido)-8-oxo-5-thia-1-azabicyclo[4.2.0]oct-2-ene-2-carboxylic acid	347.39
2		Cefalexin (6R,7R)-7-[[2-(2-amino-2-phenylacetyl)amino]-3-methyl-8-oxo-5-thia-1-azabicyclo[4.2.0]oct-2-ene-2-carboxylic acid	454.51
3		Cefradine (6R,7R)-7-[[2-(2-amino-2-(1-cyclohexa-1,4-dienyl)acetyl)amino]-3-methyl-8-oxo-5-thia-1-azabicyclo[4.2.0]oct-2-ene-2-carboxylic acid	455.47
4		Cefazolin 3-[(5-methyl-1,3,4-thiadiazol-2-yl)sulfanylmethyl]-8-oxo-7-[(2-(tetrazol-1-yl)acetyl)amino]-5-thia-1-azabicyclo[4.2.0]oct-2-ene-2-carboxylic acid	349.41

Stern-Geary method [12] used for the determination of corrosion current is performed by extrapolation of anodic and cathodic Tafel lines. Then j_{corr} was used for calculation of inhibition efficiency and surface coverage (θ) as follows [13]:

$$\% \text{ IE} = [1 - (j_{\text{corr (inh)}}/ j_{\text{corr (free)}})] \times 100 \quad (1)$$

$$\theta = [1 - (j_{\text{corr (inh)}}/ j_{\text{corr (free)}})] \quad (2)$$

where, $j_{\text{corr (free)}}$ and $j_{\text{corr (inh)}}$ are the corrosion current densities in the absence and presence of inhibitor, respectively.

The potentiodynamic current-potential curves were recorded by changing the electrode potential automatically from -500 to 500 mV with scanning rate 5mVs^{-1} . All measurements were conducted using an electrochemical measurement system (Volta Lab 21) comprised of a PGZ 100 potentiostat, a PC and Voltmaster 4 version 7.08 software for calculations. All the experiments were carried out at 25 ± 1 °C by using ultracirculating thermostat and solutions were not deaerated to make the conditions identical to weight loss measurements. The procedure adopted for the polarization measurements was the same as described elsewhere [14]. Each polarization was run three times and corrosion potentials and corrosion currents were reproducible within ± 5 mV and ± 1 $\mu\text{A cm}^{-2}$ respectively. The AC impedance measurements were carried out in the frequency range $10^5 - 5 \times 10^{-1}$ Hz with amplitude 10 mV peak-to-peak using ac signals at the open potential circuit. All measurements were performed using potentiostat/galvanostat Gamry PCI 300/4 connected to computer. A corrosion software model EIS 300 was employed. The experimental impedance were analyzed and interpreted on the basis of the equivalent circuit.

3. RESULTS AND DISCUSSION

3.1. Potentiodynamic polarization measurements

Figure 1 represents the potentiodynamic polarization curves for iron in 1 M HCl with and without the addition of compound 4 as an example of the studied compounds. Similar curves were obtained for other three compounds (not shown). The corrosion kinetic parameters such as corrosion current density (j_{corr}), corrosion potential (E_{corr}), and Tafel slopes β_a and β_c of different inhibitors derived from these Figures are given in Table (2). In all investigated compounds the inhibition efficiencies increase with increasing the concentration of these compounds. Addition of all molecules shifts the corrosion potential slightly in the positive direction without an appreciable change in β_a and β_c values. This suggests that the added compounds do not change the mechanism of iron dissolution and hydrogen evolution reactions and the inhibitors decrease both reactions by surface coverage. The polarization resistance (Table 2) values showed an increase in the presence of inhibitors and also increases with increasing the concentration.

On the basis of the experimental data, it is not difficult to deduce that in 1 M HCl these compounds act as mixed-type inhibitors. The order of decreased inhibition efficiency of all inhibitors at different concentrations is: $4 > 2 > 3 > 1$

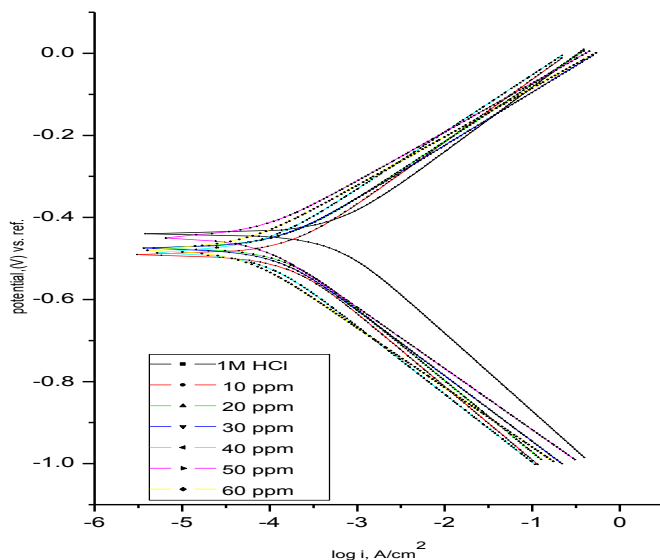


Figure 1. Potentiodynamic polarization curves for iron in 1.0 M HCl in the absence and presence of different concentrations of inhibitor (4) at 25 °C.

Table 2. The effect of concentration of compounds (1-4) on the free corrosion potential (E_{corr}), corrosion current density (j_{corr}), Tafel slopes (β_a , β_c), polarization resistance (R_p) degree of surface coverage (θ) and the inhibition efficiency (% IE,) for the corrosion of iron in 1 M HCl at 25 °C.

Comp.	Conc. ppm	$-E_{corr}$, mV(SCE)	j_{corr} , $\mu A\ cm^{-2}$	β_c , mV dec ⁻¹	β_a , mV dec ⁻¹	R_p , $\Omega\ cm^2$	θ	%IE	
								j_{corr}	R_p
Blank	0	440.3	534	190	157	70	0.00	0.00	00.0
1	10	478.8	436	186	161	106	0.180	18.0	33.9
	20	479.4	280	178	152	127	0.470	47.0	44.9
	30	484.4	279	177	153	128	0.476	47.6	45.3
	40	476.5	259	180	153	138	0.510	51.0	49.3
	50	474.0	248	181	152	145	0.536	53.6	51.7
	60	494.3	243	175	155	147	0.547	54.7	52.4
2	10	482.5	468	191	167	83	0.123	12.3	15.6
	20	475.2	442	186	165	86	0.172	17.2	18.6
	30	472.3	250	168	143	134	0.532	53.2	47.8
	40	474.0	234	179	139	158	0.562	56.2	63.2
	50	476.1	223	176	150	332	0.582	58.2	78.9
	60	479.7	169	140	137	432	0.871	87.1	83.8
3	10	484.5	416	199	173	93	0.221	22.1	24.7
	20	483.0	403	185	162	97	0.245	24.5	27.8
	30	476.9	399	198	164	106	0.253	25.3	33.9
	40	481.9	369	195	167	116	0.309	30.9	39.6
	50	483.1	315	180	157	182	0.410	41.0	61.5
	60	472.1	196	183	150	216	0.633	63.3	67.5
4	10	491.1	138	174	139	223	0.700	70.0	68.6
	20	473.3	160	178	152	242	0.742	74.2	71.1
	30	475.4	114	160	139	270	0.787	78.7	74.1
	40	483.9	80	165	129	405	0.850	85.0	82.7
	50	447.8	71	149	139	410	0.867	86.7	82.9
	60	477.7	48	145.4	118	587	0.910	91.0	88.1

3.2. Adsorption isotherm

The establishment of adsorption isotherms describes the adsorptive behavior of inhibitor molecules which can provide important ideas to the nature of the metal inhibitor interaction. Adsorption of the organic molecules occurs as the interaction energy between molecule and the metal surface is higher than that between the water molecules and surface [15]. Basic information dealing with the interaction between the inhibitor molecule and metal surface can be provided by adsorption isotherm [16]. In order to find out the adsorption isotherm, attempts were made to fit various isotherms viz., Frumkin, Langmuir and Temkin. However, the best fit was obtained only with Langmuir adsorption isotherm (equation 3) where C/θ was plotted against concentration (C) which resulted with straight lines with slope equal to unity (Fig. 2). The equilibrium constant of the adsorption process, β , which is related to the standard free energy of adsorption (ΔG°_{ads}) by [17,18].

$$C/\theta = 1/\beta + C \tag{3}$$

$$\beta = (1/55.5) \exp [-\Delta G^{\circ}_{ads} / RT] \tag{4}$$

where ,R is the universal gas constant and T is the absolute temperature, C is the inhibitor concentration and β is the equilibrium constant of adsorption.

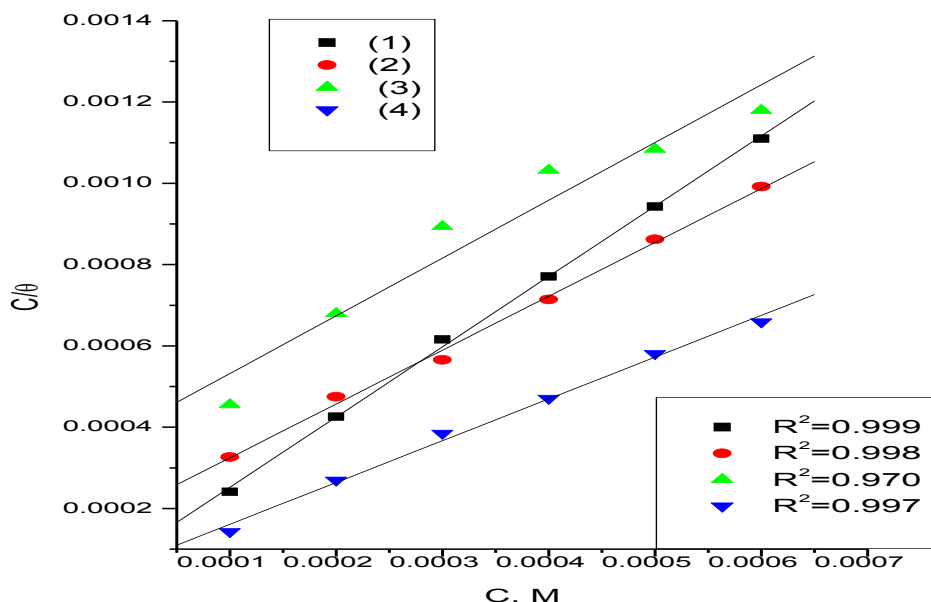


Figure 2. Langmuir adsorption isotherm plotted as (C/θ) versus C of compounds (1-4) for corrosion of iron in 1 M HCl solution at 25 °C.

Also, it is found that the kinetic– thermodynamic model of El-Awady [19] are applicable (Fig.3) which has the formula.

$$\log (\Theta / 1-\Theta)=\log K^{\wedge}+Y \log C \quad (5)$$

is agree to operate the present adsorption data. $\beta = \beta^{\circ} (1/y)$, β° is constant, and $1/y$ is the number of the surface active sites occupied by one inhibitor molecule.

The values of ΔG°_{ads} were calculated and are listed in Table 3, It is clear that the value of ΔG°_{ads} decreases in the following order: $4 > 2 > 3 > 1$ which is parallel to inhibition efficiency. The negative values of ΔG°_{ads} obtained here indicate that the adsorption process of these compounds on the iron surface is spontaneous one. The higher values of β suggested strong interaction of the inhibitors and the iron surface [20]. The increasing of β ($4 > 2 > 3 > 1$) reflects the increasing adsorption capability, due to structural formation on the metal surface.

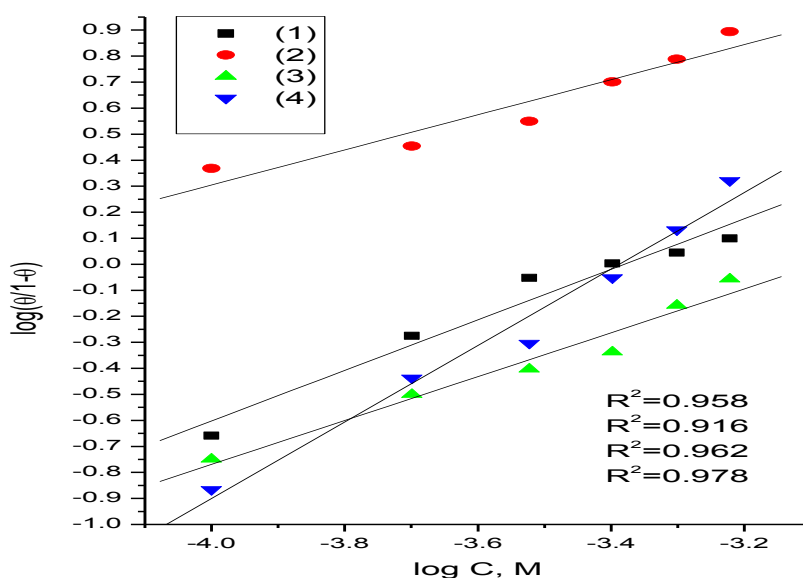


Figure 3. El-Awady et al. model plotted as $\log(\Theta/1-\Theta)$ versus $\log C$ of compounds (1-4) for corrosion of iron in 1 M HCl solution at 25 oC.

Table 3. Number of active sites ($1/Y$), Slopes of Longmuir isotherm lines, equilibrium constant of the adsorption reaction (K) and free energy of adsorption (ΔG°_{ads}) of inhibitors (1-4) on iron surface in 1 M HCl at 25 °C.

Inhibitor	Kinetic Model			Langmuir isotherm	
	1/Y	log K	$-\Delta G^{\circ}_{ads}$ kJ mol ⁻¹	K L mol ⁻¹	$-\Delta G^{\circ}_{ads}$ kJ mol ⁻¹
1	1.190	0.41	24.8	257.1	23.7
2	1.031	0.52	28.7	1261.0	27.6
3	1.492	0.48	27.1	718.2	25.5
4	0.685	0.70	38.3	520.8	28.4

3.3. Electrochemical impedance spectroscopy (EIS)

The corrosion behavior of iron in 1 M HCl solution in the absence and presence of different concentrations of compound 1 is investigated by the EIS method at E_{corr} at 25 °C after 30 min of immersion. The charge transfer resistance R_{ct} values were calculated from the difference in impedance at lower and higher frequencies from Nyquist plot (Fig. 4). Using R_{ct} , values of capacitance double layer values (C_{dl}) were computed from the Bode plot (Figs.5) by using the following equation:

$$C_{dl} = 1 / 2\pi f_{max} R_{ct} \tag{6}$$

where, f_{max} is the frequency at which the imaginary component of the impedance ($-Z_{max}$) is maximal. Similar curves were obtained for other compounds used (not shown) and the impedance parameters derived from investigations are given in Table 4. It is worth noting that the presence of inhibitor does not alter the profile of impedance diagrams which are almost semi-circle, indicating that a charge transfer process mainly controls the corrosion of iron. Deviations of perfect circular shape are often preferred to the frequency dispersion of interfacial impedance. This anomalous phenomenon is interpreted by the in homogeneity of the electrode surface arising from surface roughness or interfacial phenomena [21,22]. In fact, the presence of investigated inhibitors enhances the values of R_{ct} in the acidic solution. Values of double layer capacitance decreased in the presence of inhibitors revealing the adsorption of the inhibitor on the metal surface in the acidic solution.

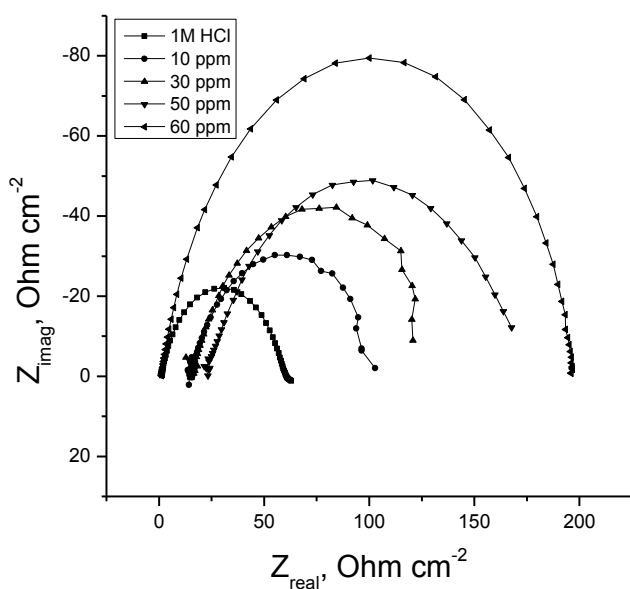


Figure 4. The Nyquist plots for iron in 1 M HCl solution in the absence and presence of different concentrations of compound (1) at 25 °C.

The inhibition efficiency and the surface coverage (θ) obtained from the impedance measurements are defined by the following relations:

$$\%IE = [1 - (R_{ct}^0/R_{ct})] \times 100 \tag{7}$$

$$\Theta = [1 - (R_{ct}^0/R_{ct})] \tag{8}$$

where, R_{ct}^0 and R_{ct} are the charge transfer resistance in the absence and presence of inhibitor, respectively.

The %IE obtained from EIS measurements are close to those deduced from polarization. The order of inhibition efficiency obtained from EIS measurements is as follows: $4 > 2 > 3 > 1$.

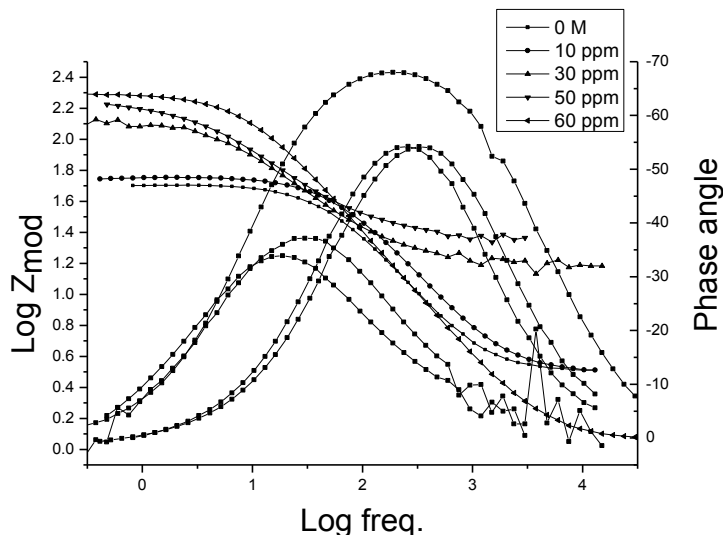


Figure 5. The Bode plots for corrosion of iron in 1 M HCl in the absence and presence of different concentrations of compound (1) a

Table 4. Electrochemical kinetic parameters obtained by EIS technique for corrosion of iron in 1 M HCl at different concentration of compounds (1-4) at 25 °C.

Comp.	Conc., ppm	Cdl μFcm^{-2}	Rct ohm	θ	IE%
Blank	0.0	86.2	52.7	0.0	0.0
1	10	81.7	71.4	0.262	26.2
	30	73.6	97.9	0.462	46.2
	50	58.7	114.5	0.540	54.0
	60	59.9	178.1	0.704	70.4
2	10	75.6	76.6	0.312	31.2
	30	51.0	111.9	0.529	52.9
	50	39.8	168.5	0.687	68.7
	60	33.2	219.1	0.760	76.0
3	10	73.3	85.0	0.380	38.0
	30	61.8	124.1	0.575	57.5
	50	41.1	165.6	0.682	68.2
	60	39.78	228.1	0.769	76.9
4	10	69.4	84.4	0.376	37.6
	30	34.77	123.9	0.575	57.5
	50	37.5	175.4	0.700	70.0
	60	30.5	295.1	0.821	82.1

3.4 Theoretical study of cephalosporin derivatives and their potential activity as corrosion inhibitors.

Quantum-chemical calculations have been widely used to study reaction mechanism and to interpret the experimental results as well as to resolve chemical ambiguities. They have also proved to be a very important tool for studying corrosion inhibition mechanism [23-26]. In recent times, Density Functional Theory (DFT) has become an attractive theoretical method because it gives exact basic vital parameters for even huge complex molecules at low cost. Furthermore, by using sophisticated computational tools, we can understand reactivity behavior of hard and soft acid-base (HSAB) theory that provide a systematic way for the analysis of the inhibitor / surface interaction [27]. Thus, the DFT has become a main source of connecting some traditional empirical concepts with quantum mechanics. Therefore, DFT is a very powerful technique to probe the inhibitor/ surface interaction and to analyze experimental data.

The effectiveness of an inhibitor can be related to its spatial molecular structure, as well as with their molecular electronic structure [28]. Also, there are certain quantum chemical parameters that can be related to the interactions metal-inhibitor. Among these, we can mention the energy of the HOMO that is often associated with the capacity of a molecule to donate electron so therefore, an increase in the value of E_{HOMO} can facilitate the adsorption and therefore the inhibition efficiency, by indicating the disposition of the molecule to donate orbital electrons to an appropriate acceptor with empty molecular orbital. In the same way low values of energy gap $\Delta E = E_{\text{LUMO}} - E_{\text{HOMO}}$ will render good inhibition efficiencies, because the energy needed to remove an electron from the last occupied orbital will be low [29]. Similarly low values of the dipole moment μ will favor us the accumulation of inhibitor molecules on metallic surface [30].

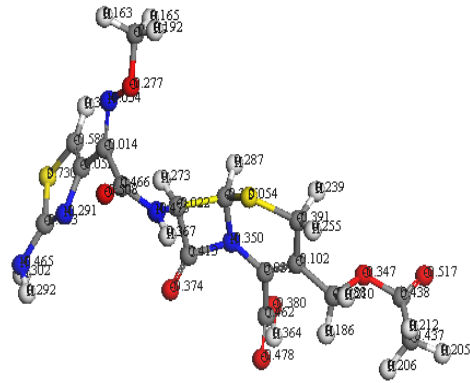
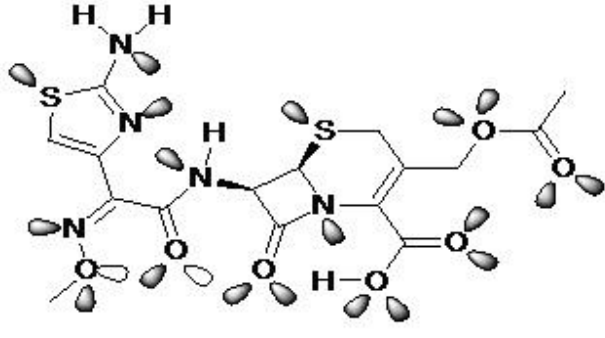
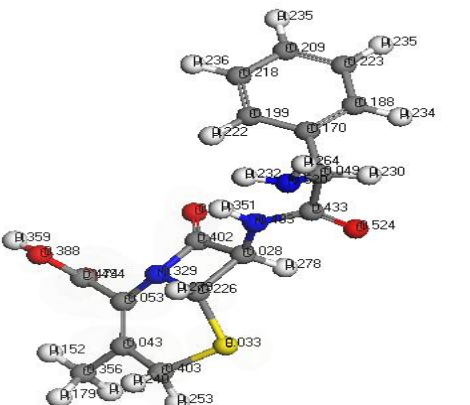
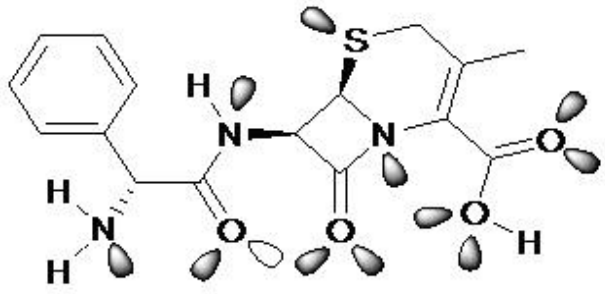
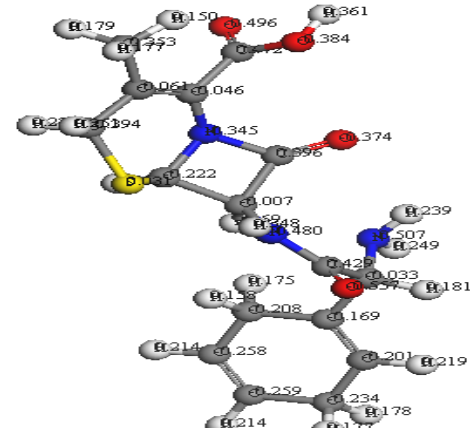
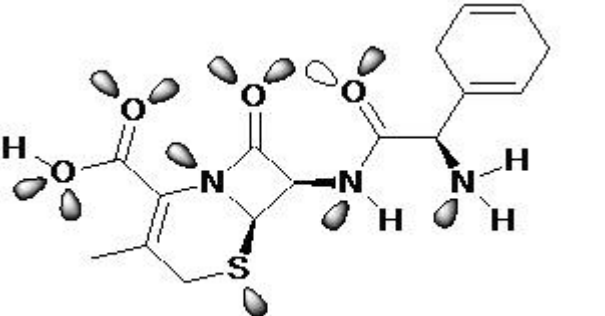
Over the past decades the semi empirical molecular orbital (MO) methods have been used widely in computational studies. In practice, these methods serve as efficient computational tools which can yield fast quantitative estimates for a number of properties.

In this study, the optimized geometries of molecules are shown in Fig (6) from PM3 electronic energy point of view. The Mulliken charge densities of investigated compounds have been calculated together with some physical characters like the E_{HOMO} , E_{LUMO} , $\Delta E = E_{\text{LUMO}} - E_{\text{HOMO}}$ and dipole moment (μ) (Table 5). The results seem to indicate that both the value of the gap energy ΔE (energy required to move an electron from HOMO to LUMO), as well as the value obtained for the dipole moment μ , favor compound (4), implying its effectiveness as a corrosion inhibitor. Low ΔE facilitates adsorption [31-33] of the molecule and thus will cause higher inhibition efficiency.

The use of Mulliken population analysis to probe the adsorption centers of inhibitors have been widely reported [34-36]. There is a general consensus by several authors that the more negatively charged heteroatom is the more it can be adsorbed on the metal surface through donor acceptor type reaction. It has also been reported that electrophiles attack molecules at sites of negative charge [37], which means that sites of ionic reactivity can be estimated from the atomic charges in the molecule.

Thus, from the values of Mulliken charge in Fig. (7), it is possible to observe that all the nitrogen and oxygen atoms present a considerable excess of negative charge. Accordingly, the investigated compounds can be adsorbed on iron surface using these centers leading to the corrosion inhibition action.

The bond gap energy ΔE increases from (1 to 4). This fact explains the decreasing inhibition efficiency in this order ($4 > 2 > 3 > 1$), as shown in Table (5) and Figs. (6&7) show the optimized structures of the four investigated compounds. So, the calculated energy gaps show reasonably good correlation with the efficiency of corrosion inhibition. Table (5) also indicates that compound (4) possesses negative E_{HOMO} that means that compound (4) adsorption occurs easily and is favored by the highest softness. The HOMO and LUMO electronic density distributions of these molecules were plotted in Fig (7). For the HOMO of the studied compounds that the benzene rings, N-atoms and O-atom have a large electron density. The data presented in Table (5) show that the calculated dipole moment decreases in the following order: ($4 > 2 > 3 > 1$)

	Charge density distribution	Structure
(1)		
(2)		
(3)		

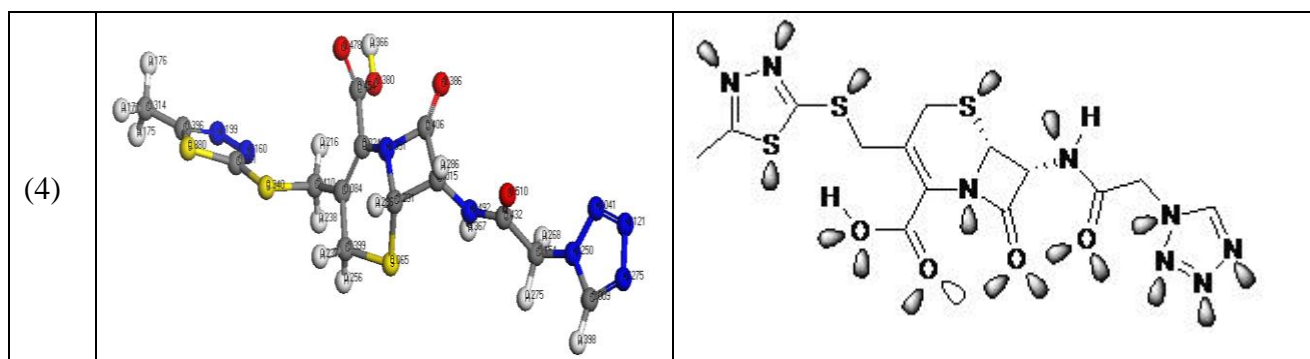


Figure 6. Optimized molecular structure of cephalosporines compounds, and the charge density distribution

	HOMO	LUMO
(1)		
(2)		
(3)		

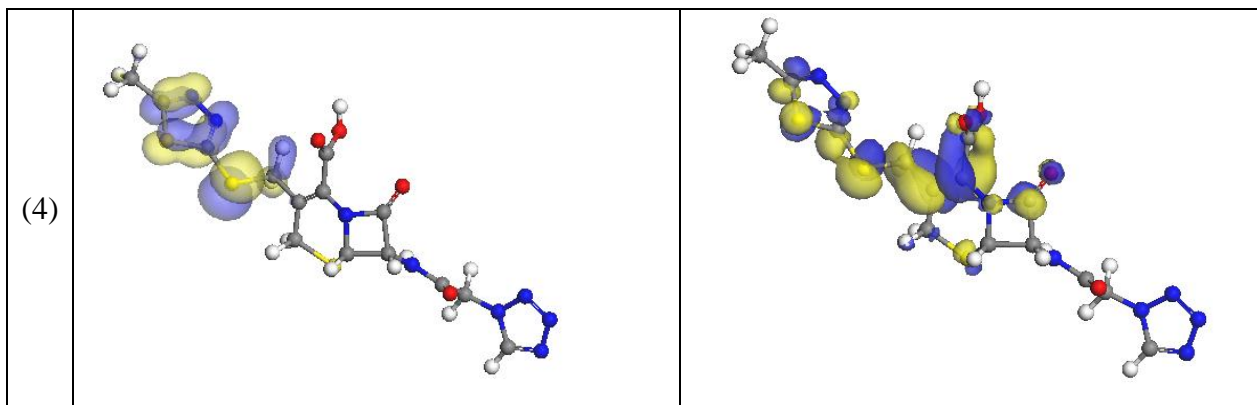
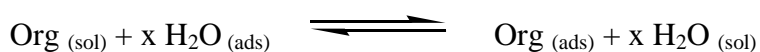


Figure 7. HOMO and LUMO structure of cephalosporin compounds.

3.5. Mechanism of corrosion inhibition

Corrosion inhibition of iron in acid chloride solution by the investigated cephalosporines drugs as indicated from potentiodynamic polarization and ac impedance was found to depend on the concentration and the nature of the inhibitor.

It is generally, assumed that adsorption of the inhibitor at the metal/solution interface is the first step in the action mechanism of the inhibitors [38-41] in aggressive acid media. In fact, the solvent molecules could also adsorb at metal/solution interface. So, the adsorption of organic inhibitor molecules from the aqueous solution can be regarded as a quasi-substitution process between the organic compounds in the aqueous phase ($\text{org}_{(\text{sol})}$) and water molecules at the electrode surface ($\text{H}_2\text{O}_{\text{ads}}$) [42].



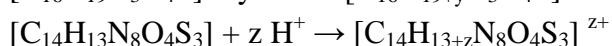
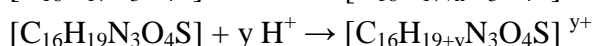
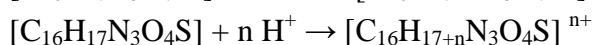
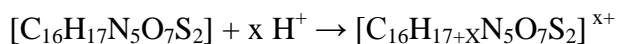
where, X is the size ratio, that is, the number of water molecules replaced by one organic inhibitor. The transition of metal/solution interface from a state of active dissolution to the passive state is attributed to the adsorption of the inhibitor molecules at the metal/solution interface, forming a protective film. The rate of adsorption is usually rapid and hence, the reactive metal surface is shielded from the aggressive environment [43].

Adsorption process can occur through the replacement of solvent molecules from metal surface by ions and molecules accumulated in the vicinity of metal/solution interface. Ions can accumulate at the metal/solution interface in excess of those required to balance the charge on the metal at the operating potential. These ions replace solvent molecules from the metal surface and their centers reside at the inner Helmholtz plane. This phenomenon is termed specific adsorption, contact adsorption. The anions are adsorbed when the metal surface has an excess positive charge in an amount greater than that required to balance the charge corresponding to the applied potential. Aromatic compounds (which contain the benzene ring) undergo particularly strong adsorption on many electrode surfaces. The bonding can occur between metal surface atoms and the aromatic ring of the adsorbate molecules or ligands substituent groups. The exact nature of interactions between a metal

surface and an aromatic molecule depends on the relative coordinating strength towards the given metal of the particular groups present [44].

In general, owing to the complex nature of adsorption and inhibition of a given inhibitor, it is impossible for single adsorption mode between inhibitor and metal surface.

The adsorption of these drugs can be attributed to the presence of polar N atoms and aromatic/heterocyclic rings. therefore, the possible reaction centers are unshared electron pair of hetero-atoms and π - electrons of aromatic ring. The adsorption and inhibition effect of investigated compounds in 1 M HCl solution can be explained as follows; drug molecules might be protonated in the acid solution as:



In aqueous acidic solutions, these drugs exist either as neutral molecules or as protonated molecules (cations). Four types of adsorption may take place during inhibition involving organic molecules at the metal/solution interface [45-47]:

- (1) Electrostatic attraction between charged molecules and the charged metal.
- (2) Interaction between unshared electron pairs and the metal.
- (3) Interaction of π -electrons with the metal.

A combination of the above [48]. Concerning inhibitors, the inhibition efficiency depends on several factors; such as the number of adsorption sites and their charge density, molecular size, heat of hydrogenation, mode of interaction with the metal surface and the formation of metallic complexes [49].

In general, two modes of adsorption are considered on the metal surface in acid media. In one mode, the neutral molecules may be adsorbed on the surface of iron through the chemisorption mechanism, involving the displacement of water molecules from the iron surface and the sharing electrons between the hetero-atoms and iron. The inhibitor molecules can also adsorb on the iron surface on the basis of donor-acceptor interactions between π -electrons of the aromatic ring and vacant d-orbitals of surface iron atoms. In second mode, since it is well known that the iron surface bears positive charge in acid solution [50] so, it is difficult for the protonated molecules to approach the positively charged iron surface (H_3O^+ /metal interface) due to the electrostatic repulsion. Since Cl^- ions have a smaller degree of hydration, thus they could bring excess negative charges in the vicinity of the interface and favor more adsorption of the positively charged inhibitors molecules, the protonated inhibitor adsorb via electrostatic interactions between the positively charged molecules and the negatively charged metal surface. Thus, there is a synergism between adsorbed Cl^- and protonated inhibitors thus; we can conclude that inhibition of iron corrosion in 1M HCl is mainly due to electrostatic interaction. The decrease in inhibition efficiency with rise in temperature supports electrostatic interaction.

4. CONCLUSIONS

Antibacterial cephalosporin is found to be good inhibitors for iron corrosion in 1 M HCl. The inhibition is accomplished by adsorption of cephalosporin molecules on to the iron electrode surface without changing the mechanism of partial corrosion reactions. Adsorption of these compounds follows Langmuir adsorption isotherm. In 1 M HCl these antibacterial cephalosporins act as mixed-type inhibitors. EIS measurements indicate the single charge transfer process controlling the corrosion of iron. The order of the inhibitive effect has been found to be: 4 > 2 > 3 > 1.

References

1. G. Schmitt, *Br. Corr. J.*, 19 (1984) 165.
2. A. Doner, R. Solmaz, M. Ozcan and G. Kardas, *Corros. Sci.* 53(2011)2902.
3. M. Abdallah, Basim H. Asghar^a, I. Zaafarany and A. S. Fouda, *Int. J. Electrochem. Sci.* 7(1) (2012) 282.
4. M. Abdallah, Sh. T. Atwa, N. M. Abdallah, I. M. El-Naggar and A. S. Fouda, *Anti Corrosion Methods and Materials*, 58(1), (2011) 31
5. S. M. A. Hosseini, M. Salari, E. Jamalizadeh, S. Khezripoor and M. Seifi, *Mater. Chem and Phys.* 119(2010)100.
6. M. Abdallah, H. E. Megahed and M. S. Motae, *Mater. Chem and Phys.*, 118, (2009) 111
7. M. Abdallah, E. A. Helal and A. S. Fouda, *Corros. Sci.*, 48 (2006) 1639.
8. X. Li, S. Deng and H. Fu, *Corros. Sci.*, 53(2011)3241.
9. K. S. Jacob, G. Parameswaran, *Corros. Sci.*, 52(2010)224.
10. M. Abdallah, I. Zaafarany, K. S. Khairou and M. Sobhi, *Int. J. Electrochem. Soc.*, 7(2) 1564-1579 (2012)
11. G. Subramanian, K. Balasubramanian and P. Sridhar, *Corros. Sci.*, 30 (1990) 1019.
12. M. Stern and A. I. J. Geary, *J. Electrochem. Soc.*, 104 (1957) 56.
13. F. Bentiss, C. Jama, B. Mernari, H. El Attari, L. El Kadi, M. Lebrini, M. Traisnel and M. Lagrenee, *Corros. Sci.*, 51 (2009) 1628.
14. F. Bentiss, M. Lagrenee, M. Traisnel and J. C. Hornez, *Corros. Sci.*, 41(1999)789
15. E. McCafferty, in: Leidheiser, Jr. (Ed), (1979) 279.
16. F. Bentiss, M. Traisnel, N. Chaibi, B. Mernari, H. Vezin and M. Lagrenee, *Corros. Sci.*, 44(2002) 2271.
17. M. Kliskic, J. Radosevic and S. Gridic; *J. Appl. Electrochem.*, 27 (1997) 947
18. A. M. S. Abdel and A. El- Saied; *Trans. Soc. Adv. Electrochem. Sci. Technol.*, 16(1981)197.
19. Y. A. El-Awady and A. I. Ahmed, *J. Ind. Chem.*, 24A (1985) 601.
20. E. E. Oguzie, *Corros. Sci.*, 49 (2007) 1527.
21. S. L. F. A. DA Costa and S. M. L. Agostinho, *Corros. Sci.*, 45(1989)472.
22. H. Shih and H. Mansfeld, *Corros. Sci.*, 29 (1989)2271.
23. J. Bessone, C. Mayer, K. Tuttner, W. J. Lorenz; *Electrochim. Acta*, 28 (1983) 171.
24. F. Bentiss, M. Traisnel and M. Lagrenee, *Corros. Sci.*, 42 (2000) 127.
25. M. G. Hosseini, *Electrochim. Acta*, 52 (2007) 3650.
26. I. B. Obot and N. O. Obi-Egbedi, *Colloids and Surface A: Physicochem. Eng. Aspects*, 330 (2008) 207.
27. I. B. Obot and N. O. Obi-Egbedi, *Surf. Rev. Lett.*, 15(6) (2008) 903.
28. I. B. Obot, N. O. Obi-Egbedi and S. A. Umoren, *Corros. Sci.*, 51 (2009) 276.
29. J. Cruz, T. Pandiyan and E. Garcia-Ochoa, *J. Electroanal. Chem.*, 583 (2005) 8.
30. H. Ashassi-Sorkhabi, B. Shaabani and D. Seifzadeh, *Electrochim. Acta*, 50 (2005) 3446.
31. N. Khalil, *Electrochim. Acta*, 48 (2003) 2635.
32. J. Fang and J. Li, *J. Mol. Struct. (THEOCHEM)*, 593 (2002) 179.

33. N. K. Allam, *Appl. Surf. Sci.*, 253 (2007) 4570.
34. F. Kandemirli and S. Sagdina, *Corros. Sci.*, 49 (2007) 2118.
35. G. Bereket, C. Ogretic and C. Ozsahim, *J. Mol. Struct., (THEOCHEM)*, 663 (2003) 39.
36. M. Ozcan, I. Dehri and M. Erbil. *Appl. Surf. Sci.*, 236 (2004) 155.
37. D. Wang, S. Li, Y. Ying, M. Wang, H. Xiao and Z. Chem, *Corros. Sci.*, 41 (1999) 1911.
38. M. H. Kelestemur and T.K. Chaki, *International Journal of fatigue* 23 (2001) 169.
39. L.W. Tsay, M.C. Young, C. Chen, *Corros. Sci.* 45 (2003) 1985.
40. L.W. Tsay, Y.C. Liu, M.C. Young, D. Y. Lin, *Mater. Sci. Eng. A* 374 (2004) 204.
41. L.W. Tsay, M.C. Young, F.Y. Chou, R.K. Shiue, *Mater. Chem. Phys.* 88 (2004) 348.
42. M.Sahin, S.Bilgic and H.Yilmaz, *Appl. Surf. Sci.*, 195(2002)1.
43. C.Y.Cho, L.F.Lin and D.D.Macdonald, *J.Electrochem. Soc.*,128(1981)1187)
44. I.M. Ritchie, S. Bailey and R. Woods, *Adv. Colloid interface Sci.*, 80(1999) 183
45. Gihan I. Youssef, M.SC. thesis Cairo Univ., Egypt (1992).
46. P. W. Athins, *Physical Chemistry*, Oxford University Press, Oxford, 5th ed., (1994), p. 922.
47. B.B. Damaskin, O.A. Petrij and V.V. Batrakov, *Adsorption of Organic Compounds on Electrodes* Plenum Press, New York, 86 (1971).
48. D.Schweinsberg, G.George, A.Nanayakkara and D.Steinert, *Corros. Sci.*, 28(1988) 33.
49. A.S.Fouda, M.N. Moussa, F.I. Taha and A.I.El-Neanaa, *Corros. Sci.*, 26(1986) 719.
50. G.N.Mu, T.P. Zhao, M.Liu and T.Gu, *Corros.*, 52(1996) 853.